

## Non-destructive analysis of pre-hispanic gold objects using energy-dispersive X-ray fluorescence

R. CESAREO, G.E. GIGANTE

*Dipartimento di Energetica, Università di Roma "La Sapienza",  
Rome, Italy*

J.S. IWANCZYK

*Xsirius Inc., Marina del Rey, CA 90292, USA*

M.A. ROSALES

*Departamento de Física y Matemáticas  
Universidad de las Américas-Puebla  
Apartado postal 100, Sta. Catarina, Mártir, 72820 Puebla, Pue., México*

M. ALIPHAT\*

*Subdirección de Servicios Académicos  
Instituto Nacional de Antropología e Historia  
México, D.F., México*

AND

P. AVILA

*Instituto Nacional de Investigaciones Nucleares  
Apartado postal 18-1027, México, D.F., México*

Recibido el 16 de marzo de 1993; aceptado el 16 de noviembre de 1993

**ABSTRACT.** The technique used in the present work is that of energy dispersive X-ray fluorescence (EDXRF), where monoenergetic  $\gamma$ -rays from a portable radioisotopic  $^{241}\text{Am}$  source were used to stimulate X-rays emission from the sample. These secondary photons were analyzed with the help of an experimental  $\text{HgI}_2$  detector working at room temperature. In particular, in this paper we present the results of the application of the above technique to the analysis of pre-hispanic jewelry from several regions of Mexico.

**RESUMEN.** La técnica utilizada en el presente trabajo es la de fluorescencia de rayos X con dispersión en la energía (EDXRF). Se emplearon los rayos  $\gamma$  monoenergéticos de una fuente radioisotópica portátil de  $^{241}\text{Am}$  para estimular la emisión de rayos X en la muestra. Estos fotones secundarios se analizaron con un detector de  $\text{HgI}_2$  que se encuentra en etapa experimental, y que funciona a temperatura ambiente. En este artículo presentamos los resultados obtenidos al aplicar la técnica descrita al análisis de un lote de joyería prehispánica de diversas regiones de México.

PACS: 07.85.+n; 29.30.Kv; 29.40.Pe

---

\*Present address: Department of Archaeology, University of Calgary, Calgary, Alberta, Canada.

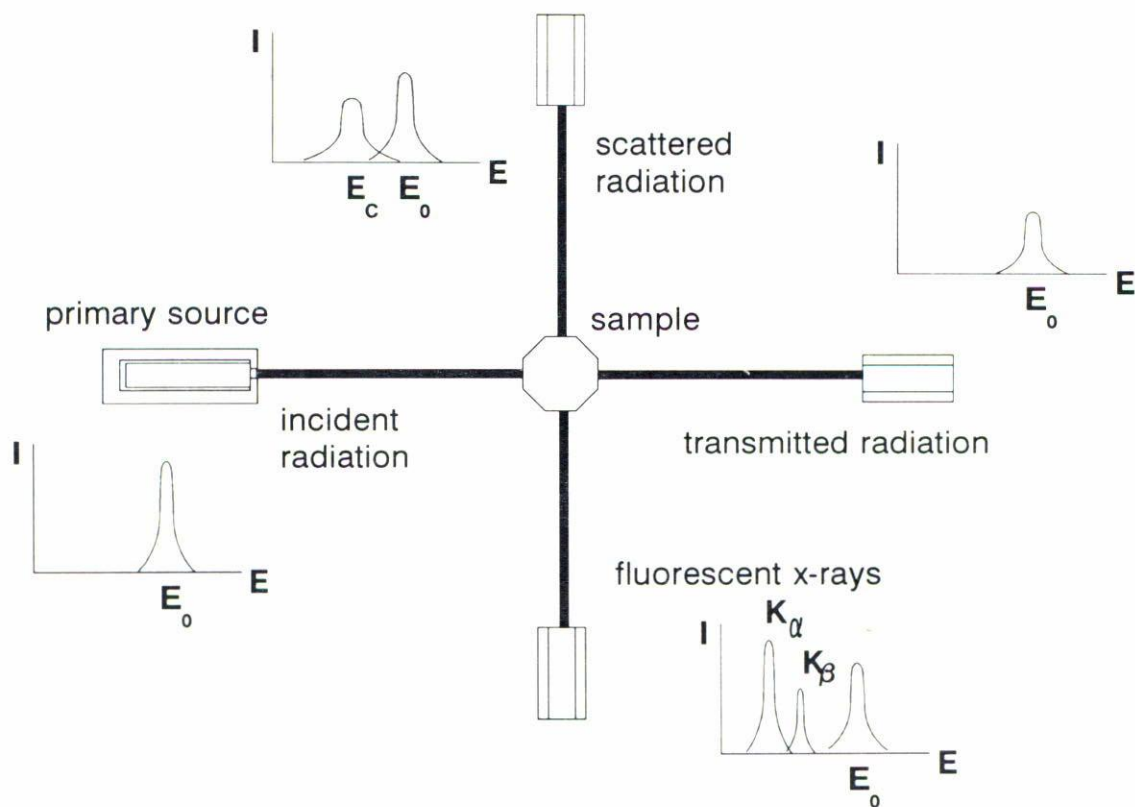


FIGURE 1.

1. INTRODUCTION

When a sample is irradiated with keV photons, some of them are absorbed through the photoelectric effect mechanism, some other are elastically or inelastically scattered and, finally, a small fraction of the incident photon beam is capable of crossing the sample without interacting with it. When different X-rays photon detectors are set up around the sample, as in Fig. 1, they collect the outgoing photons of different light-matter interaction mechanisms. The energy and intensity of the photonic peaks supply relevant information on a given mechanism and on the cross section associated with it [1,2]. Hence, valuable information about the chemical elements present in the sample can be obtained through the analysis of the characteristic X-ray photons emitted by such sample acting as a secondary photon source [3].

For an incident monochromatic X-rays beam of intensity  $I_0$ , the outgoing spectrum contains [1]:

- a) A peak of intensity  $I_0 \exp(-\mu\chi)$  centered at the energy  $E_0$  in the transmission mode as detected by the detector  $D_2$  in Fig. 1. Since  $\chi$  denotes the sample thickness, it is clear that as it increases the transmitted beam becomes less significant.
- b) A peak centered at  $E_0$  as detected by  $D_1$  in Fig. 1, due to elastic scattering.

- c) A peak around the energy  $E_c$ , as detected by  $D_1$ , coming from atomic Compton-like scattering.
- d) Several peaks around the transition energies characteristic of the chemical elements in the sample, as detected by  $D_3$ . These peaks are produced via the photoelectric effect.

The experimentally obtained spectrum becomes more complex due, mainly, to two effects:

- i) the preferential annihilation of photons in some specific region of the spectrum by absorption within the sample (self-absorption), and
- ii) the emission of secondary radiation due to multiple interactions (multiple scattering, multiple photoelectric interaction or a mixture of these);

and the relevance of these two effects increase with the sample dimensions.

Also, it is important to mention that the detection system has an energy resolution and this determines how close two peaks may be in order to be distinguished. The Compton profile can be further complicated due to:

- 1) A *geometry dependent factor*, which increases the width of the peak by an amount that can be approximated as

$$\Delta G = E_0[1 + \gamma(1 - \cos \theta_{\max})]^{-1} - E_0[1 + \gamma(1 - \cos \theta_{\min})]^{-1},$$

where  $\gamma = E_0/m_0c^2$ ,  $\theta$  is the angle between the incident and the scattered photons, and  $\theta_{\min}$  and  $\theta_{\max}$  are the minimum and maximum values of the angle between the sample's plane and the detection direction.

- 2) *Electron momentum distribution in the scatterer*. If this were the only factor degrading the energy resolution the whole width at half height (FWHM) of the pulse height distribution would be

$$\Delta C \propto J(p_z, Z),$$

where the threshold  $p_z$  for the momentum component along the incident beam depends on the energy and the scattering angle, and the function  $J(p, Z)$  is called the *Compton profile*.

## 2. XRF ANALYSIS

As mentioned earlier, when a sample is irradiated with X- or  $\gamma$ -rays of the appropriate energy, characteristic secondary X-rays photons are emitted from such sample. This, in turn, allows the identification of the chemical elements in it. The intensities are proportional to the concentration of a given element. In general, a spectrum consists of: elastically scattered photons, photons coming from Compton scattering and X-rays photons characteristic of the sample.



In the limit of infinite thickness, that is the general case when liquids, alloys, metals, etc. are analyzed, in whose case the dimensions are greater than a few tenths of a mm, such a thickness is also greater than the reach of the secondary radiation and, in this case, the *flux* of photons produced by fluorescence, by coherent and Compton dispersion is given, respectively, by [1]

$$N_a = \frac{N_0 K \omega_a \mu_{\text{pha}}(E_0)(1 - 1/J_a) c_a}{\mu_t(E_0) + \mu_t(E_a)}, \quad (1)$$

$$N_{\text{coh}} = \frac{N_0 k \mu_{\text{coh}}}{2\mu_t(E_0)}, \quad (2)$$

$$N_C = \frac{N_0 K \mu_C}{\mu_t(E_0) + \mu_t(E_C)}, \quad (3)$$

where  $N_a$  (photons/cm<sup>2</sup>s) is the fluorescent photon flux density (number of photons per unit area and time) of X-rays of element  $a$ ,  $N_0$  (photons/cm<sup>2</sup>s) is the incident photon flux density,  $K$  is a geometrical factor,  $\omega_a$  is the fluorescent yield of element  $a$  in the shell of interest,  $1 - 1/J_a$  is the branching factor that corresponds to the intensity of X-rays in the line of interest over the total X-rays intensity,  $c_a$  (%) is the concentration (% by weight) of element  $a$ ,  $m$  (g/cm<sup>2</sup>) is the mass per unit area of the sample,  $\rho$  (g/cm<sup>3</sup>) is its density,  $\mu_t(E)$  (cm<sup>2</sup>/g) is the total mass absorption coefficient of the sample at energy  $E$ ,  $\mu_{\text{pha}}(E_0)$ , (cm<sup>2</sup>/g) is the photoelectric absorption coefficient of element  $a$  at incident energy  $E_0$ , and  $\mu_{\text{coh}}$  and  $\mu_C$  (cm<sup>2</sup>/g) are the absorption coefficients of the sample for coherent and incoherent scattering, respectively.

The first of the above equations allows one to relate the photons flux density of X-rays produced by fluorescence and the concentration of a given element. In this way, the composition of the sample is determined by EDXRF. In Eq. (1) the parameters  $\omega_a$ ,  $\mu_{\text{pha}}$ ,  $1 - 1/J_a$ ,  $\mu_t(E_0)$  and  $\mu_t(E)$  either are known or can be theoretically calculated. The factor  $N_0 K$  can be experimentally determined analyzing a reference standard sample and, hence,  $c_a$  can be evaluated if the value of  $N_a$  is measured. Alternatively, a calibration curve for the generic  $a$  element can be constructed with the help of a sufficiently large number of reference samples containing that element.

X-rays fluorescence is a simple non-destructive analytical technique which, for analysis of "infinitely thick" samples as in the case of gold analysis, is characterized by a minimum detectable limit of the order of 0.1% or less, depending on the source (energy and intensity) and on the element to be analyzed.

### 3. EXPERIMENTAL SETUP

The apparatus for EDXRF employed for the analysis of ancient prehispanic gold objects is characterized by:

1. A 45 mCi <sup>241</sup>Am radioactive source, which emits 59.6 keV  $\gamma$ -rays. This source, provided by the Instituto Nacional de Investigaciones Nucleares of Mexico, is able to

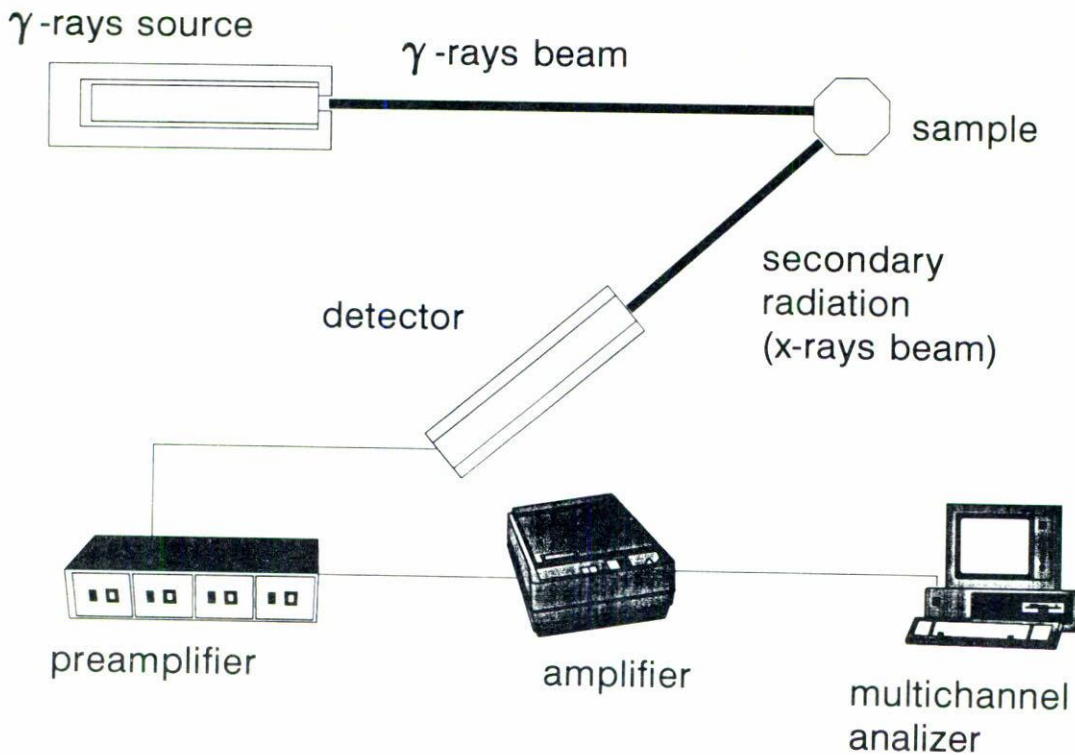


FIGURE 2.

induce photoelectric effect in Ag ( $K$ -shell), Au ( $L$ -shell), Cu ( $K$ -shell) and eventually in other elements if present at concentration levels larger than about 0.1%.

It should be observed that the excitation is more efficient for elements having the energy of the photoelectric discontinuity close to 59.6 keV (for example Ag) than for elements like Cu with a discontinuity far away from that energy.

2. A HGI<sub>2</sub> room temperature semiconductor detector provided by Xsirius Inc. This detector, which can also be partially cooled by the Peltier effect, is characterized by very reduced dimensions and an energy resolution of about 250 eV at 6.4 keV (if Peltier cooled, a little larger than at room temperature), comparable with nitrogen cooled semiconductor detectors.

3. A multichannel board for PCs.

Such equipment can be used everywhere, including places in which no liquid nitrogen is available, like museums or excavation areas. These characteristics make the equipment very suitable for *in situ* archaeological analysis.

#### 4. PRE-HISPANIC GOLD OBJECTS ANALYSIS

Among the important application of the EDXRF technique the ones related to Archeology are relevant [2]. In particular, we present the results obtained for a set of gold objects

TABLE I.

Aztec				Mixtec			
Code	Au (%)	Ag (%)	Cu (%)	Code	Au (%)	Ag (%)	Cu (%)
PUL126-1	83.0	17.0	0.0	P7-2390A	82.2	16.0	1.8
PUL126-2	77.0	23.0	0.0	P7-2390B	71.4	27.0	1.6
08716612	79.0	20.0	1.0	P7-2390C	70.4	28.0	1.6
U8716612	78.0	22.0	0.0	P7-2390D	78.2	19.0	2.8
PCO1P23A	92.8	6.0	1.2	P7-2317A	71.9	24.0	4.1
PCO1P23B	92.3	6.5	1.2	P7-2317B	77.0	20.0	3.0
DOML25-1	79.0	21.0	0.0	P7-2317C	65.0	25.0	10.0
DOML-2	83.0	17.0	0.0	DT7459A	97.0	3.0	0.0
B252890A	81.7	18.0	0.3	DT7459B	97.0	3.0	0.0
B252890B	79.0	21.0	0.0	N7-3058A	88.0	12.0	0.0
PC2P127A	73.0	27.0	0.0	N7-3058B	86.0	12.0	2.0
PC2P127B	73.0	27.0	0.0	D7-2405A	84.3	13.0	2.7
FCB054	77.2	20.0	2.8	D7-2405B	81.9	15.0	3.1
FCB054B	79.3	18.0	2.7	R7-3426A	62.2	31.0	6.8
CM02-1*	71.0	29.0	0.0	R7-3426B	71.5	24.0	4.5
CM02-2*	68.0	32.0	0.0	A7-2391A	77.4	21.0	1.6
BPEOP55A*	71.0	29.0	0.0	A7-2391B	80.0	20.0	0.0
BPEOP55B*	65.0	35.0	0.0	B7-2404A	67.6	31.0	1.4
P17CR-A*	72.0	28.0	0.0	B7-2404B	86.0	14.0	0.0
C252938A	63.6	30.0	6.4				
C252938B	81.0	19.0	0.0				

\* The analysis of this sample is affected by a larger error due to the poor counting statistics.

Mayan			
Code	Au (%)	Ag (%)	Cu (%)
P5-1516A	94.6	4.2	1.2
P5-1516B	94.7	3.5	1.8
C5-3853A	96.7	3.3	0.0
C5-3853B	96.0	4.0	0.0
L51517A1	96.5	3.5	0.0
L51517C1	97.2	2.8	0.0
ML53855	96.5	3.5	0.0

produced by some of the Mexican pre-hispanic cultures and currently kept in the Museo del Templo Mayor and the Museo de Antropología of Mexico City.

A summary of the data is presented in Table I, where the objects are listed according to their origin and their composition as revealed by the EDXRF technique. It must be mentioned that, in many cases, there is not any other experimental evidence about chemical composition of the jewels as to compare our values. In our case we must include a relative



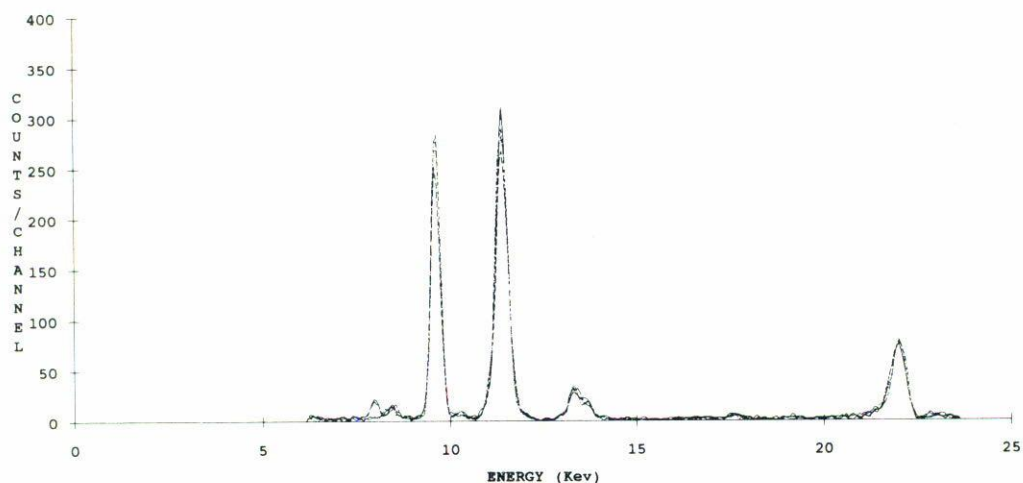


FIGURE 3.

uncertainty of about 6 to 7%, comparable to the one obtained with other techniques applied to the determination of gold, silver and copper contents [4-7]. Finally, in Fig. 3 we present a typical spectrum obtained in the present work.

## 5. CONCLUSION

From a scientific point of view, the purpose of this analysis has been twofold: First, it has served as a test for the new HGI<sub>2</sub> detector, the advantages of which are evident since its performance at room temperature has permitted to use it in the study of masterpieces and some other hardly transportable objects. On the other hand, with this work we have given the first step towards the establishment of a database necessary for the identification of the objects under study, that is obviously important for archaeological classification and preservation purposes.

It must also be mentioned that, although the present results were obtained by means of Eqs. (1), (2) and (3). we are currently engaged in the problem of the determination of weight fractions through the use of fundamental physical parameters only. This means that the number of incident photons and the geometrical factors would not appear in the final expressions for the (relative) weight fractions for the different chemical elements involved.

## ACKNOWLEDGEMENTS

This work was partially supported by CONACYT, Mexico. Some of the authors (R.C., G.E.G. and J.S.I.) were supported in this work by the NATO grant CRG900130.

## REFERENCES

1. R. Cesareo, A.L. Hanson, G.E. Gigante, L.J. Pedraza, and S.Q.G. Mahtaboally, *Phys. Rep.* **213** (1992) 117, and references therein.
2. R. Cesareo, G.E. Gigante, J.S. Iwanczyk, and A. Dabrowsli, *Nucl. Instr. Meth. Phys. Res.* **A322** (1992) 583.
3. E.F. Aguilera, R. Policroniades, and M.E. de la Rosa, *Rev. Mex. Fís.* **39** (1993) 110.
4. R. Cesareo, *Nucl. Instr. Meth.* **179** (1981) 545.
5. A. Hartmann, *Antiquity* **44** (1972) 22.
6. E.R. Caley, *Analysis of ancient metals*, Pergamon Press, London (1964).
7. C.M. Dozinelli, in *Modern methods of analysis of copper and its alloys*, Elsevier, Amsterdam (1963) 103.